**A COMBINED CATHODOLUMINESCENCE AND MICRO-RAMAN STUDY OF PLANAR DEFORMATION FEATURES IN QUARTZ.** A. Gucsik[1,2], T. Okumura[3], M. Kayama[3], H. Nishido[3], K. Ninagawa[4] [1]Department of Earth and Planetary Materials Science, Graduate School of Science, Tohoku University, Aoba 6-3, Aramaki, Aoba-ku, Sendai, 980-8578, Japan (E-mail: ciklamensopron@yahoo.com); [2]Konkoly Observatory of the Hungarian Academy of Sciences, H-1121, Budapest, Konkoly Thege Miklós út 15-17., Hungary; [3]Research Institute of Natural Sciences, Okayama University of Science, 1-1 Ridai-cho, Okayama, 700-0005, Japan; [4]Department of Applied Physics, Okayama University of Science, 1-1 Ridai-cho, Okayama, 700-0005, Japan

**Introduction:** According to Goltrant et al. [1,2] the formation mechanisms of the Planar Deformation Features (PDFs) of the shocked quartz in nature might be explained by the pressure dependence of the shear modulus of quartz for various planes and directions. The Si-O-Si bonds are more easily broken, allowing the corresponding atoms to move towards energetically more favorable positions. This progressive rearrangement leads to the formation of a new structure (dense amorphous silica lamellae). The transformation occurs very rapidly, as it is driven by the front of the shock wave. This explanation predicts that the density of PDFs should markedly increase with shock intensity [1,2].

The question of whether shock metamorphic effects may modify the luminescent nature of quartz under subsequent compression has been addressed in a pioneering study of Boggs et al. [3]. Here, we report the first systematic experiments that investigate the effect of shock-induced amorphization on the electronic transitions in the high-pressure phase transitions. Up to now, phase transition studies of quartz have been mostly conducted on high-pressure polymorph of quartz (i.e., coesite, stishovite), not typical of shock-induced microstructures in quartz as it is found in the target rocks of the terrestrial impact craters. It was noted that quartz from intrusive igneous and high-grade metamorphic rock shows darker purple-blue CL, whereas quartz from low-grade metamorphic rocks exhibit reddish-brown CL, and that shocked quartz from the Cretaceous-Tertiary (K/T) boundary exhibits CL colors similar to those of low-grade metamorphic quartz [4]. CL properties of shocked quartz have been described from various shock metamorphic environments such as terrestrial impact structures [5,6] and shock recovery experiments [7]. These authors studied characteristic behaviors of variable-intensity CL accompanied by zoning, healed fractures, domain structures, complex shears and planar microdeformations from different source rocks, using a combined scanning electron microscopy (SEM)-CL fabric-analysis technique. Our results not only contribute to an improved understanding of the formation conditions of PDFs in quartz (e.g., during a meteorite impact), but also reveal the potential for the shock-induced amorphization in new electronic transitions in the amorphous phase of minerals.

**Experimental Procedure:** The Raman spectra were obtained using a Thermo Nicolet Almega confocal micro-Raman spectrometer with a Nd:YAG (20 mW at 532 nm) laser excitation system and a cooled CCD detector at 223 K. The spectral measurements were carried out at 1 μm intervals over a sectional area of 30 μm square with a 1 sec exposure time. It was confirmed that peak positions did not change during the Raman measurements. The analytical area was 30 x15 micrometers with analytical 450 (30x15=450) points for 3D Raman spectroscopy. For 3D Raman imaging analysis of quartz the integrated intensity at 459 $cm^{-1}$ peak of each analytical point was used. 3D-Raman spectral images could be taken automatically with specialized software (Atlμs).

SEM-CL imaging and CL spectral analyses were performed on selected polished thin sections (from Ries meteorite crater, Germany) coated with a 20-nm thin film of carbon in order to avoid charge build-up. SEM-CL images were collected using a Scanning Electron Microscope (SEM-JEOL 5410LV), equipped with a CL detector (Oxford Mono CL2), which comprises an integral 1200 grooves/mm grating monochromator attached to a reflecting light guide with a retractable paraboloidal mirror. Operating conditions for all SEM-CL investigations as well as SEM and backscattered electron (BSE) microscopy were 15 kV accelerating voltage and beam current 2.0 nA at room temperature, 0.05 nA at low temperature. For the measurements at low temperatures, a cryostage temperature-controlled down to –195 °C with liquid nitrogen and embedded heater was employed. A lower beam current was required at low temperature due to the temperature quenching effect, since CL emission of quartz significantly increases below –80 °C. CL spectra were recorded in the wavelength range of 300-800 nm, with 1 nm resolution by the photon counting method using a photomultiplier detector, Hamamatsu Photonics R2228.

The CL spectral data as a function of wavelength (nm) were corrected by total instrument response, which was determined using a calibrated quartz halogen lamp (Eppley Laboratory Co.), because of consid-

erable sensitivity variation of the PMT (Hamamatsu R2228) in the measurement wavelength range and exclusion for two instrumental anomalies of the grating, called "Wood's anomalies", recognized as the inflection point in a curve. Corrected CL spectral data were converted into the energy space (eV) from a relationship between energy (eV) and wavelength (nm), which is energy (eV) = 1239.8/ wavelength (nm) [8]. These spectra are fitted by Gaussian function, because CL emission band in energy space is Gaussian distribution [9]. For the evaluation of temperature quenching effect on the quartz, luminescence efficiency (η) derived from integrated intensities of a Gaussian compornet was assumed 0.9 at maximum value in measured temperature range.

**Results and Discussion:** *Scanning Electron Microscope-Cathodoluminescence observations:* PDFs of quartz from Ries impact crater are discernible in the optical and Scanning Electron Microscope (Secondary Electron) microscope images occurring as multiple sets of closely spaced (3-8 μm), narrow ( <1-3 μm), parallel planar regions (Fig. 1a). CL-dark parallel lines corresponding to PDFs appear in the otherwise CL-bright image of the shocked quartz grain (Fig. 1a). PDFs show bright BSE signal, which corresponds to more dense material than luminescent matrix of quartz.

*Raman spectra:* The SEM-CL image of PDFs refers to the Raman analyzing area representing three intersecting sets of non-luminescent dark lines (Fig. 1a). The 2-D Raman imaging of the PDFs shows a stripe pattern suggesting layer-type structure comprised of high and low crystalline parts indicated the presence of crystalline and amorphous phases in the PDFs of quartz (Fig. 1b). A single quartz (colorless, optical grade) crystal from Minas Gerais, Brazil, was employed for spectral correction and used as a reference material for this study. Main Raman peaks of this quartz are: 128, 204, 264, 355, 464, 508, 808 and 1079 $cm^{-1}$. Raman spectra of shocked quartz exhibit a dominant peak at around 459 $cm^{-1}$, whereas typical high-quartz has a sharp and intense peak at 464 $cm^{-1}$, which can be assigned to O-Si-O stretching vibrational mode (Fig. 1c). This frequency shift is related to a distortion of structural configuration such as formation of high density diaplectic $SiO_2$ glass and/or amorphization associated with the occurrence of glass-filled PDFs. The 3D Raman mapping of the PDFs also shows the high and low crystalline parts indicated the amorphous infilling material in the host quartz grain (Fig. 1d).

*Cathodoluminescence (CL) spectrum:* CL spectrum of shocked quartz contains two broad bands centered at 450 to 650 nm, which are assigned to presence of defect centers on, e.g., $SiO_4$ groups (Fig. 2). The dominant observed defects occur in the short-range order involving the slightly distorted $SiO_4$ tetrahedra, which are common to both the crystalline and amorphous $SiO_2$ structures [10]. We observed that the CL emission, which is enhanced at a lower temperature (–192 °C), several hundred times more intense than that at room temperature (25 °C) due to temperature quenching effect (Fig. 3). It gives a strong broad peak in the blue region with doublet apexes at 455 and 465 nm, which could be assigned to intrinsic emission bearing on the E'1 and E'2 centers [10] .

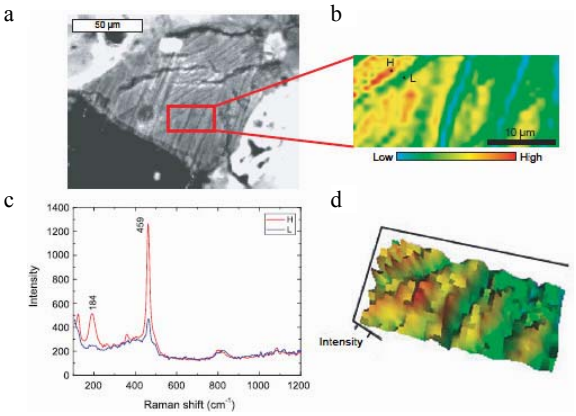


***Figure 1.*** *Scanning Electron Microscope-Cathodoluminescence image (a) of three sets of well-developed PDFs in a quartz sample from the Ries impact structure. 2D (b), Raman spectra (c), and 3D (d) Raman images exhibit variations of low (L) andhigh (H) intensity areas corresponding the occurrence of amorphous material (low intensity parts).*

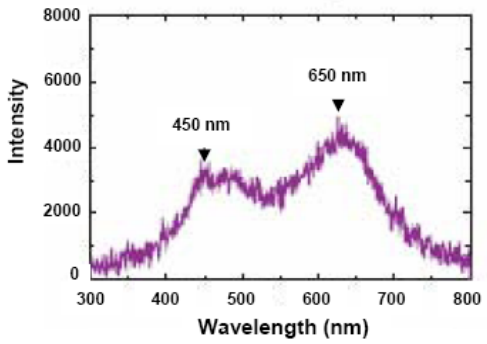


***Figure 2.*** *CL spectrum of shocked quartz obtained at room temperature with PDFs shows a doublet peak, which is centered at 450 and 500 nm (defect centers on, e.g., $SiO_4$ groups).*

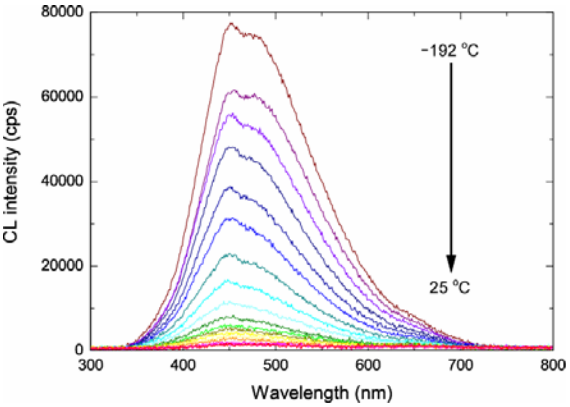


***Figure 3.*** *CL spectra of unshocked and shocked quartz samples at various temperatures.*

*Temperature quenching effect of shocked quartz.* The probability of non-irradiative transitions depends on temperature and is represented as equation (1):

$$s\exp(\varepsilon/kT) \quad (1)$$

,where s is frequency factor, k is Boltzmann constant, and T is absolute temperature (K). Therefore, the luminescence efficiency (η) is proportional to the probability of radiative, A, and that of non-radiative transitions. With the activation energy (eV) for temperature quenching, ε, the temperature dependence of the luminescence efficiency can be described as equation (2):

$$\eta = A/(A + s\exp(\varepsilon/kT)) \quad (2)$$

To quantitatively evaluate temperature dependence of CL intensity obtained by spectral measurements on a sample temperature, activation energy for temperature quenching was estimated using the equation (2) by assuming Mott-Seitz model. From modification of equation (2), the analysis using Arrhenius plot of ln[(1/η)-1] against 1/T leads to estimation of activation energy in temperature quenching processes for shocked and unshocked quartz. Activation energy is determined from the slope of least-square linear fit. Two activation energies (ε) for shocked quartz from Ries crater are 0.072 ~ 0.085 eV in the range from −180 to −30 °C. Compared to the shocked quartz, the unshocked quartz (hydrothermal origin) exhibits two temperature quenching processes, where ε is 0.032 eV up to −110 °C and 0.222 eV above −110 °C. High-quartz (beta-quartz) shows almost same quencing process as Ries quartz. In this case, for the further studies, we have to apply a new analytical model for quartz using multiple-quantum-well structures proposed by Vening et al. [11].

*Non-luminescent nature of PDFs*. It was noted that the energy difference between the top of the valence band (VB) and the bottom of the conduction band (CB) in quartz is 3.1 eV **[**3**]** , which is equivalent to approximately 400 nm. Thus, even a small amount of energy from the electron beam causes electrons to enter the CB, from where they then fall back and move randomly through the crystal structure until they encounter a trap or recombination center [12]. As electrons return to lower energy states via traps, they can produce photons with energies in the visible portion of the spectrum, or even in the near-infrared region. If they return directly from the CB to the VB, they emit photons in the UV region of the spectrum [9,13] note that quartz is an insulator mineral, in which the band gap between conduction and valence bands is too large for simple thermal excitation to promote electrons from lower-energy states to the higher-energy states [8]. A band gap (BG) exists between valence band (VB) and conduction band (CB). The shock-induced amorphization can cause affect to electronic transition process in defect centers correlated to CL emission, as follows. The amorphous infilling material of PDFs can modify the energy level arrangement of electron traps existing in the BG, which indicates that the luminescence process does not operate or is very inefficient. This means the amorphous material causes new closely spaced energy levels and the electrons can easily return to the ground state with the emission of a succession of low-energy photons, or by losing energy to the lattice in the form of heat (phonon emission-tiny energetic vibration packages leading to heat of the sample. This confirms the observations of Boggs et al. [3] and agrees with the conclusions obtained from our Raman spectroscopic observations. Alternatively, the non-luminescent areas must either be essentially free of traps or recombination centers (i.e., photons in the visible light range are not emitted if traps are absent).

**Conclusions and Summary:** In summary, the displacive phase transformation of quartz (i.e., trigonal-hexagonal transition at low temperature and high pressure) occurred in the PDFs has small symmetry and electronic structure-breaking displacements of atoms resulting non-radiative processes in the luminescence emission. This indicates that the non-luminescence of the PDFs will increase with decreasing temperature and increasing shock pressure. We noted that the combination of SEM-CL and micro-

Raman techniques is a useful tool for the evaluation of the shock stages and identification of shock-induced microdeformations in the shock-deformed minerals, especially for the rock-forming minerals

**References:** [1] Goltrant O. et al. (1991) *Earth Planet. Sci. Lett., 102,* 103-115. [2] Goltrant O. et al. (1992) *Physics Earth Planet. Inter., 74*, 219-240. [3] Boggs S. et al. (2001) *Meteoritics & Planet. Sci. 36,* 783-793. [4] Owen M.R. and Anders H.M. (1988) *Nature 334,* 145-147. [5] Ramseyer K. et al. (1992) *Tectonophysics 216*, 195-204 (1992). [6] Seyedolali A. et al. (1997) *Geology 25,* 787-790. [7] Gucsik A. et al. (2003) *Meteoritics & Planet. Sci. 38,* 1187-1197. [8] Nasdala L. et al. (2002) *Chem. Geol., 191*, 121-140. [9] Yacobi, B.G. and Holt, D.B. (1999) Cathodoluminescence Microscopy of Inorganic Solids. Springer, p. 308. [10] Kalceff M.A.S. et al. (2000) In Cathodoluminescence in Geosciences (eds. Pagel M., Barbin, V., Blanc, Ph. and Ohnenstetter, D.), Springer, p. 193-224. [11] Vening et al. (1993) Phys. Rev. B 48, 2412–2417. [12] Hayward C.L. (1998) In: Cabri L.J. and Vaughan D.J. (eds) Modern Approaches to Ore and Environmental Mineralogy. Mineralogical Association of Canada Short Course Series, 27, 269-325. [13] Gaft M. et al. (2005) Modern Luminescence Spectroscopy of Minerals and Materials. Springer, p. 356.

.